Low-field diamagnetic response of the superconducting phases in UPt_3

1991 J. Phys.: Condens. Matter 3 3517

(http://iopscience.iop.org/0953-8984/3/20/013)

J. Phys.: Condens. Matter 3 (1991) 3517–3525. Printed in the UK

Low-field diamagnetic response of the superconducting phases in UPt_3

E Vincent†, J Hammann†, L Taillefer‡§, K Behnia‡¶, N Keller‡ and J Flouquet‡

† Service de Physique du Solide et de Résonance Magnétique, CEN Saclay, 91191 Gif-sur-Yvette Cédex, France

‡ Centre de Recherches sur les Très Basses Températures, CNRS, BP 166 X, 38042 Grenoble Cédex, France

Received 16 October 1990

Abstract. By measuring the gradual disappearance of diamagnetism in a single crystal of UPt_3 upon warming through the superconducting transition in a constant magnetic field, we have investigated the temperature dependence of a characteristic field H_{c1}^*, closely related to the superconducting lower critical field H_{c1}. The amplitude of the applied field ranged from 1 to 60 Oe, for directions along the *b*- and the *c*-axis of the hexagonal structure. A distinct change in the slope of $H_{c1}^*(T)$ is observed for both directions, at a temperature which coincides well with the lower transition detected by specific heat within the superconducting regime. It is further found that the initial slope of H_{c1}^* is roughly isotropic, in contrast with the marked anisotropy of dH_{c2}/dT, and that the Meissner effect is extremely small despite the long electronic mean free path.

1. Introduction

On the basis of several experimental results, the field–temperature phase diagram of superconducting UPt_3 is thought to be subdivided into three separate regions or phases (for a recent review see Taillefer *et al* [1]). In particular at low fields, two clear discontinuities in the heat capacity [2] reveal unambiguously the presence of a phase transition within the superconducting regime. In zero magnetic field, this lower transition at T_c^- occurs 55 mK below the onset of superconductivity from the normal phase at $T_c^+ \simeq 0.5$ K. A measurement of the thermal expansion [3] along the hexagonal axis of the crystal structure has shown that T_c^- will increase and T_c^+ decrease under *c*-axis compression, suggesting empirically that the two transitions are the result of a splitting. Moreover, recent pressure studies [4, 5] indicate that this splitting is related to the weak antiferromagnetic order in UPt_3, which develops below 5 K with moments lying in the hexagonal basal plane [6]. The separation ΔT_c between the two transitions was seen to vanish under an applied hydrostatic pressure of 3.7 kbar [4] and the Bragg scattering from the antiferromagnetic order above T_c was suppressed

§ Present address: Laboratoire Louis-Néel (CNRS), BP 166 X, 38042 Grenoble Cedex, France.

¶ Present address: Département de Physique de la Matière Condensée, Université de Genève, 24 Quai Ernest Ansermet, CH-1211 Genève 4, Switzerland.

0953-8984/91/203517+09$03.50

under pressure and found to extrapolate to zero at about 3 kbar [5]. The parallel disappearance of the splitting ΔT_c and the antiferromagnetic order, at a pressure which otherwise affects the electronic properties very little, points convincingly to the coupling of superconducting and magnetic order parameters and supports the idea that the latter is responsible for lifting the degeneracy of T_c. This idea was introduced and developed in a model of broken hexagonal symmetry [7–9], based on an analogy with superfluid ^{3}He and its field-induced splitting of the doubly degenerate transition to phase A. The original assumption of this, and of all other models currently applied to UPt_3, is the superconducting nature of the transition at T_c^-, i.e. that it involves a change in the superconducting order parameter. It is possible to test this assumption experimentally by investigating the low-field diamagnetic response near T_c^-. In this article, we present the results of such an investigation, which show that an increase in the slope of $H_{c1}(T)$ occurs at T_c^-, consistent with an increase in condensation energy of the superconducting state, pointing to the appearance of a new superconducting order parameter at the lower transition. In addition, new insight is gained into the behaviour of vortices in this compound.

2. Experimental details

The single crystal used in this study was well characterized by an earlier measurement of the de Haas–van Alphen effect [10] which yielded a direct estimate of the electronic mean free path of 1300 Å, for a representative orbit on the Fermi surface. The crystal was cut from a polycrystalline ingot prepared in a UHV furnace by horizontal float zoning from high-purity starting material [10]. Its residual resistivity ρ_0 is estimated to be 0.4–0.5 $\mu\Omega$ cm (along the c-axis) from measurements on neighbouring crystals. Its shape is that of a slab of thickness 0.5 mm with the b- and c-axis in the plane of the slab whose perimeter is approximately circular with diameter 2 mm. The demagnetizing factor is estimated to be of order 0.17, for a field in the b–c plane, with a negligible b–c anisotropy. In the present experiments, the magnetic field was applied in two directions: b and c.

The variation with temperature of the DC magnetization of UPt_3 was measured in a SQUID magnetometer as the change in flux linking a pair of compensated coils, one of which contained the sample. The sample was cooled by conduction through a copper braid fixed onto the mixing chamber of a dilution refrigerator. The temperature was estimated from the resistance of a Ge thermometer fixed some distance away from the sample. A small temperature gradient was thus thought to have been present between sample and thermometer, and can be responsible for a slight shift in the temperature scale (of order 4 mK) observed when the crystal was rotated from the b- to the c-axis. However, within each of the two series of measurements, the reproducibility was established to be better than 1.5 mK. The absolute calibration of the magnetometer is known within ±10%, a margin which corresponds to an uncertainty in the exact position of the sample inside the coils. A constant and steady magnetic field was obtained by trapping the flux produced by an external solenoid inside a concentric lead shield. The residual field was of the order of 50 mOe.

Data were recorded in the following way. The sample was cooled from above (550 mK) to below (200 to 300 mK) the superconducting transition in zero field; at the lower temperature, the magnetic field (1 to 60 Oe) was applied. The temperature was then increased slowly in steps of 1 mK up to 550 mK under constant field, and

the corresponding variation of the diamagnetic shielding signal was recorded ('ZFC' curves). This procedure yields the flux penetration as a function of increasing temperature, starting from a magnetically shielded state. In addition, for some values of the field, the flux expulsion due to the Meissner effect was also recorded by decreasing the temperature under the same constant field starting at 550 mK ('FC' curve).

3. Results

The magnetization as a function of temperature has been measured for a series of fixed values of the applied field H_a namely from 1 to 60 Oe in steps of 5 Oe for both crystal directions. Figure 1 displays a few typical ZFC curves obtained with the field along the *b*-axis (similar curves were obtained for the *c*-axis). For $H_a = 1$ Oe, we also present the FC curve, or Meissner effect, measured immediately after (magnified by 10). The diamonds are a subset of the raw experimental points, The comparison of FC and ZFC curves shows to what extent the diamagnetic response of this sample, very pure from the point of view of electron motion, is irreversible. Indeed, the Meissner effect is extremely small for both crystal directions, corresponding at best to 3% of full screening (see figure 1), and furthermore, it decreases with increasing field by a factor 10 in going from 1 to 60 Oe.

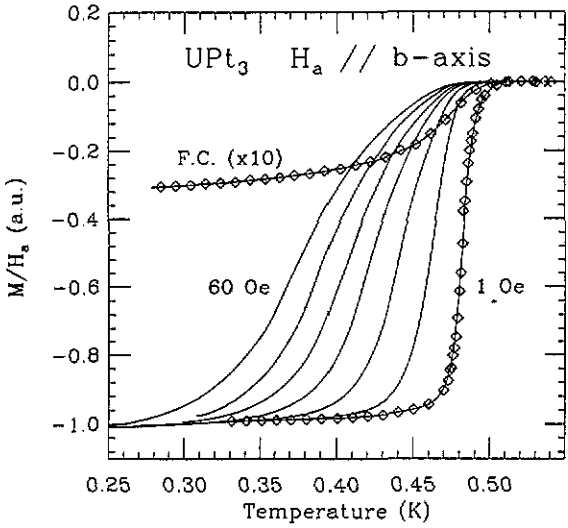

Figure 1. Temperature dependence of the magnetization for fields of 1, 10, 20, 30, 40, 50 and 60 Oe applied along the *b*-axis. The set of full curves (through the data points) corresponds to flux screening, with the temperature having been increased after the field was applied at the lowest temperature. The diamonds shown are a subset of the data points taken at 1 Oe, including the flux expulsion, or Meissner effect, measured upon cooling the sample in the field (labelled F.C.; magnified by a factor 10).

The demagnetizing effects were not large, since the field was only applied in the plane of the UPt_3 slab. Nevertheless, the data were corrected by estimating the internal field H_i, assumed to be uniform and given by

$$H_i = H_a - 4\pi N M \qquad \text{(cgs units)} \tag{1}$$

where M is the magnetization and $N = 0.17$ for both crystal directions b and c. The corrected 'internal susceptibility' $\chi_i = M/H_i$ thus reads:

$$4\pi\chi_i = \frac{4\pi\chi_a}{1 - 4\pi N\chi_a} \qquad (2)$$

where $\chi_a = M/H_a$. Within the $\pm 10\%$ uncertainty on the overall calibration, the susceptibility is found to reach its full value of $4\pi\chi_i = -1$ at low temperature for both directions. In a separate experiment performed on another sample of the same batch, absolute amplitude measurements corrected in this way yield the same results, i.e. a complete magnetic shielding of the sample volume after cooling in zero field, and an extremely weak flux expulsion upon cooling in the field. In view of this, for subsequent analysis the normalization factor was adjusted slightly so that $4\pi\chi_i(T) = -1$ exactly, at the low-temperature plateau.

We aim to determine the temperature dependence of H_{c1} or, in the present conditions, the temperature $T_{c1}(H)$ at which the first vortex penetrates in the sample for different values of the field. This occurs when $M(T)$ begins to depart from its constant low T value. However, this departure is initially governed by flux entering at the edges of the sample and does not represent the behaviour of the bulk. For this reason, we have chosen to avoid that initial region of the magnetization curve and to define, as a characteristic temperature, the point at which the shielding has come down by some small fraction (say by 10 to 20%). The penetration of flux in the corresponding volume fraction may be sensitive to a slight variation in the critical current density with temperature but, as will be seen, the precise fraction chosen makes little qualitative difference. The corresponding characteristic field, denoted H^*_{c1}, is therefore closely related to the proper H_{c1} and, in particular, will have a temperature dependence similar to it, although it should be an overestimate of the magnitude of H_{c1}. For the analysis to follow, a criterion of 15% 'loss-in-shielding' is used, namely $4\pi\chi_i(H, T_{c1}) = -0.85$. This particular criterion yields approximately the same values of T_{c1} as those obtained from extrapolating the tangent at the point of inflexion onto the base line.

The result of using such a definition is plotted as H_i against T in figures 2(a) and (b) for a field parallel to the b- and c-axis, respectively. The salient feature is a change in the slope of $H^*_{c1}(T)$ for both field directions, occurring at $T = T_0$. Beyond that point, H^*_{c1} increases more rapidly than hitherto, as can in fact be inferred by direct inspection of the raw data in figure 1. Numerical estimates are derived from two linear fits: one at low fields (1 to 20 Oe) and another at high fields (30 to 70 Oe), displayed in figure 2. Their intersection yields the coordinates (T_0, H_0) of the change in slope, or 'kink', with an error bar corresponding to the uncertainty in the choice of data points to be included in the fits. The results are listed in table 1. The observed kinks show up at 53 ± 6 and 49 ± 6 mK below $T_{c1}(H \to 0)(\equiv T_c)$, as an increase of 1.40 ± 0.05 and 1.32 ± 0.06 in the slope $\mathrm{d}H^*_{c1}/\mathrm{d}T$, for $\boldsymbol{H}_a \parallel \boldsymbol{b}$ and $\boldsymbol{H}_a \parallel \boldsymbol{c}$, respectively. A change in criterion from 20 to 10% does not affect the presence of the kink, nor does it modify either the ratio of slopes or ΔT, within the error bars of table 1. It causes $-\mathrm{d}H^*_{c1}/\mathrm{d}T$ to decrease by some 15% and T_c to decrease by approximately 5 mK.

The rationale of our analysis is the following: if one examines whether there is a change of slope in $H^*_{c1}(T)$ in the vicinity of the established lower transition at $T = T_c^-$ by applying a linear fit to the low-field data and a separate linear fit to the high-field data, both fits being satisfactory, one finds the two resulting slopes to be quite different, and furthermore, the top one to be greatest. The change in slope at T_0 is

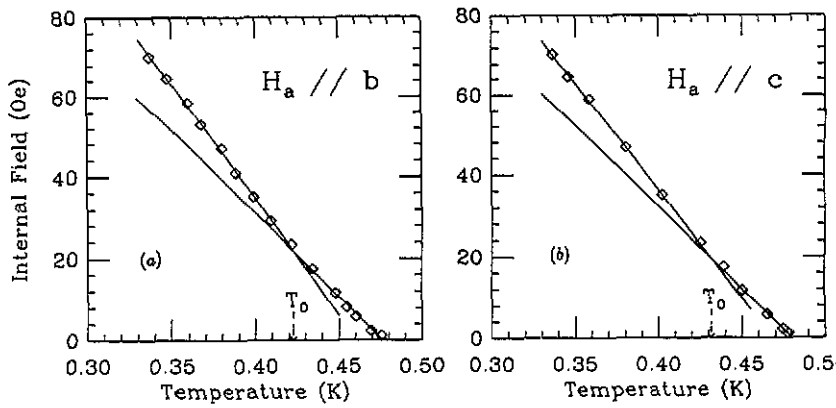

Figure 2. (*a*) Lower critical field H^*_{c1} (defined in the text) against temperature for $\boldsymbol{H} \parallel \boldsymbol{b}$. The full lines are two separate linear fits to the data at low and high fields, respectively. Note the change in slope by a factor 1.40 at a temperature $T_0 = 423$ mK, namely 53 mK below $T_c(H \to 0)$. (*b*) Same for $\boldsymbol{H} \parallel \boldsymbol{c}$. A change in the slope of $H^*_{c1}(T)$ is also observed in this direction, estimated at 49 mK below T_c.

Table 1. Characteristics of the $H^*_{c1}(T)$ curve for the two field directions, derived from the linear fits in figure 2. The coordinates of the kink are (T_0, H_0). T_c is the extrapolation of the low-field data to $H = 0$ and $(\mathrm{d}H^*_{c1}/\mathrm{d}T)_{H\to 0}$ is the corresponding slope. Also given are the separation $\Delta T = T_c - T_0$ and the ratio of the slopes below and above T_0. Units are mK and Oe.

Direction	T_c	T_0	ΔT	H_0	$-(\mathrm{d}H^*_{c1}/\mathrm{d}T)_{H\to 0}$	Ratio
$\boldsymbol{H}_a \parallel \boldsymbol{b}$	476 ± 1	423 ± 6	53 ± 6	22 ± 3	0.41 ± 0.02	1.40 ± 0.05
$\boldsymbol{H}_a \parallel \boldsymbol{c}$	480 ± 1	431 ± 6	49 ± 6	20 ± 3	0.40 ± 0.02	1.32 ± 0.06

small but resolved reliably due to the low scattering of our data. This is a result of the procedure chosen: a measurement at constant field takes advantage of the rapid variation of χ with T to determine $T_{c1}(H)$, as opposed to the relatively slow deviation of M from linearity as a function of increasing H in an isothermal experiment, hence the greater sensitivity.

4. Discussion

4.1. Meissner effect

The extremely small Meissner effect observed in this and other high-quality crystals of UPt_3 [11] corresponds to a remarkably weak expulsion of flux, attributed to a strong pinning of the vortices. Since the electronic mean free paths in these samples are long, between 1000 and 2000 Å (from de Haas–van Alphen studies [10]), pinning does not result from a high density of impurities. Moreover, the vortices appear to move rather easily under the influence of a Lorentz force: from electrical conduction

experiments performed on whiskers of comparable residual resistivity [12], a transverse field ($H \perp J$) of order 1 kOe was found to broaden significantly the resistive transition even in the presence of an electrical current density as low as $J \simeq 2$ A cm^{-2}. So it appears that in UPt_3 the pinning force can be weak compared with a small Lorentz force, yet very effective when it comes to vortex expulsion, and whatever the pinning centres are, they have little effect on electron motion.

4.2. Anomaly at T_0

The anomaly at T_0 must be placed in the context of other thermodynamic properties, for example by locating it with respect to the two transition temperatures T_c^- and T_c^+ derived from the specific heat $c(T)$ [2, 3], the thermal expansion coefficient $\alpha(T)$ [3] and the sound velocity $v(T)$ [13], all measured in similar crystals of UPt_3. These three separate quantities exhibit two distinct discontinuities as a function of temperature (both positive in c/T, both negative in v and of opposite sign in α [1]), the midpoints of which define T_c^- and T_c^+. The resulting values are given in table 2, where it is seen that they all agree within experimental accuracy, yielding a separation $\Delta T_c (\equiv T_c^+ - T_c^-)$ of 56 ± 5 mK. In the same table, we compare T_0 and T_c derived from the present magnetic measurements to the thermodynamic T_c^- and T_c^+, respectively. The correspondence is evident and T_0 occurs precisely at the lower transition, i.e. ΔT_c below the onset of superconductivity. The coincidence of the increase in dH_{c1}/dT at T_0 with the thermodynamic anomaly at T_c^- leads us to conclude that the former is indeed due to a gain in condensation energy associated with the transition evidenced by the latter.

Table 2. Comparison of the characteristic temperatures T_0 and T_c derived from the present H_{c1} study with the two transition temperatures T_c^- and T_c^+ observed in specific heat, thermal expansion and sound velocity measurements on three similar crystals. Due to the difference in the method of definition, the various absolute values for T_c^- and T_c^+ may not all coincide exactly. Nevertheless, the separation $\Delta T_c = T_c^+ - T_c^-$ obtained from all techniques is the same within experimental uncertainty. This confirms that the increase in dH_{c1}^*/dT at T_0 corresponds indeed to the transition at T_c^- evidenced in thermodynamic measurements. Units are mK.

	Sample	T_c^-	T_c^+	ΔT_c	Reference
Specific heat	1	434 ± 2	490 ± 2	56 ± 3	[2]
Thermal expansion	2	442 ± 4	494 ± 3	52 ± 5	[3]
Sound velocity	2	434 ± 4	495 ± 3	61 ± 5	[13]
$H_{c1}(H_a \parallel b)$	3	423 ± 6	476 ± 1	53 ± 6	This work
$H_{c1}(H_a \parallel c)$	3	431 ± 6	480 ± 1	49 ± 6	This work

It must be stressed that this interpretation can realistically be made only within such a quantitative comparison between magnetic and thermodynamic measurements. The H_{c1} anomalies observed by Zhao *et al* [14] in isothermal DC measurements of $M(H)$, as those observed earlier by Shivaram *et al* [15] in high-frequency AC measurements, are found to occur well below T_c^-, i.e. approximately $3\Delta T_c$ below T_c^+. These anomalies are therefore difficult to interpret in terms of the established phase diagram of UPt_3.

The most natural explanation for a gain in condensation energy is the appearance of a new superconducting order parameter associated with the lower transition. In this sense, our H_{c1} study provides positive evidence in favour of a superconducting

mechanism for T_c^-, something which was often assumed given the absence of any indication for either a magnetic or a structural ordering in this temperature range. (Note in this respect that, within experimental accuracy, no anomaly was detected in the magnetization $M(T)$ itself (see figure 1) at $T = T_0 = 423$ mK.) Conversely, it would seem that any theoretical model for the phase diagram of UPt_3 based on a multiplicity of superconducting phases will predict an increase in $|dH_{c1}/dT|$ at T_c^-. Within a model of this kind, where the two superconducting phases in zero field are taken to arise from the split transition of a two-dimensional order parameter whose degeneracy is lifted by a field that breaks the hexagonal symmetry, Hess *et al* [8, 16] have calculated $H_{c1}(T)$ in the Ginzburg–Landau (GL) approach. They find that the magnitude of the increase in $|dH_{c1}/dT|$ at T_c^- depends on the two specific heat jumps $\Delta c/T$ and on two coefficients of the gradient terms in the GL expansion. In this model, these coefficients are related to the break in the slope of the upper critical field $H_{c2}(T)$ predicted to occur in one specific direction, imposed by the symmetry-breaking field. A break in dH_{c2}/dT is well established experimentally but it is found to exist for *all* directions of the field in the basal plane [5]. If, nevertheless, we follow Hess *et al* in using the measured slope on either side of the break at H^*, namely $dH_{c2}/dT = -44$ and -64 kOe K^{-1} for $H < H^*$ and $H > H^*$ respectively [12, 17], an estimate of the relevant GL coefficients is obtained within this model, and the predicted ratio $\mathcal{R}$ of slopes below and above T_c^- comes out to be $\mathcal{R}(c) = 1.72$ for $H \parallel c$ [8, 16], using $\Delta c\_T_c^+/\Delta c + T_c^- = 1.5$ [2–4]. This is considerably greater than our present result of $\mathcal{R}(c) = 1.32 \pm 0.06$.

Another difficulty with the broken-symmetry model (at least in its simplest form) is that, contrary to prediction, we find the kink in $H_{c1}(T)$ to be essentially isotropic in the b–c plane. From table 1, $\mathcal{R}(c) = 1.32$ and $\mathcal{R}(b) = 1.40$. The model yields 1.72 for the c-axis, and either 1.30 or 1.91 for the b-axis [16] (depending on the direction of the symmetry-breaking field) using the values of dH_{c2}/dT and Δc previously quoted. In fact, the results of Zhao *et al* [14] obtained with a spherical sample yield, within the error bars, the same H_{c1} curve for all three high-symmetry directions a, b and c (below 60 Oe). This difficulty may be removed if the condition of macroscopic broken-symmetry is relaxed, as in the model of Joynt *et al* [18], where the coupling between magnetic and superconducting order parameters is taken to be local, limited in space to the extent of the antiferromagnetic domains, particularly small in UPt_3 [6].

4.3. Critical fields at T_c^+

Quite apart from the transition at T_c^-, and the associated anomaly at T_0, one can attempt to describe the onset of superconductivity from the normal state (at T_c^+) with the standard approach. First, the thermodynamic critical field H_c may be obtained from the relation

$$\frac{\Delta c}{T_c^+} = \frac{1}{4\pi}\left(\frac{dH_c}{dT}\right)^2_{T_c^+} \tag{3}$$

where $\Delta c \equiv c_S - c_N$ is the jump in specific heat at T_c^+. With $\Delta c/T_c^+ = 210$ mJ K^{-2} mol^{-1} [2–4], we deduce a value for the slope of H_c near T_c^+ of -788 Oe K^{-1}. Second, we define two parameters κ_1 and κ_3 using the standard relations to the upper and lower critical fields, respectively [19]

$$H_{c2}(T) = \sqrt{2}\kappa_1(T)H_c(T) \tag{4}$$

and

$$H_{c1}(T) = f(\kappa_3)H_c(T) \tag{5}$$

where

$$f(\kappa_3) \simeq [\ln \kappa_3(T)/\sqrt{2}\kappa_3(T)] \qquad \text{for } \kappa_3 \text{ large.}$$

Near T_c^+, H_{c2} is linear in T and $\mathrm{d}H_{c2}/\mathrm{d}T = -44$ Oe mK^{-1} for $\boldsymbol{H} \perp \boldsymbol{c}$ and -75 Oe mK^{-1} for $\boldsymbol{H} \parallel \boldsymbol{c}$, from specific-heat data [3, 17]. This yields $\kappa_1(T = T_c^+) = (\mathrm{d}H_{c2}/\mathrm{d}T)/(\sqrt{2}\mathrm{d}H_c/\mathrm{d}T) = 40$ and 67, for $\boldsymbol{H} \perp \boldsymbol{c}$ and $\boldsymbol{H} \parallel \boldsymbol{c}$ respectively. These are large values, suggesting that in UPt_3 the coherence length is much smaller than the penetration depth. In a one-parameter GL description where $\kappa = \kappa_1 = \kappa_3$, one would then expect the slope of H_{c1} near T_c to be very small: $-\mathrm{d}H_{c1}/\mathrm{d}T \simeq (-\mathrm{d}H_c/\mathrm{d}T)(\ln\kappa/\sqrt{2}\kappa) = 52$ and 35 Oe K^{-1}, for $\boldsymbol{H} \perp \boldsymbol{c}$ and $\boldsymbol{H} \parallel \boldsymbol{c}$ respectively. This is five to ten times smaller than the values of $-\mathrm{d}H_{c1}^*/\mathrm{d}T$ measured in this work, or in the work of Zhao *et al* [14], where a somewhat lower value of 250 Oe K^{-1} is observed. Furthermore, the large anisotropy of $H_{c2}(T)$ near T_c is not reflected in the initial slope of H_{c1}^*, which is, as previously mentioned, essentially isotropic. An alternative approach is to estimate κ_3 directly from the relationship between H_{c1} and H_c given in equation (5). From the data of table 1, the numerical solution of $f(\kappa_3)$ for small κ_3 [19] gives $\kappa_3(T = T_c^+) \simeq 2.5$; the data of Zhao *et al* yield approximately 5. Such a large discrepancy between κ_1 and κ_3, defined respectively from the slopes of H_{c2} and H_{c1} in the linear regime near T_c is most unusual. The discrepancy goes far beyond the uncertainty on the three experimentally determined critical fields, including the uncertainty on $H_{c1}(T)$. Although we do not claim to be extracting the precise absolute value of $H_{c1}(T)$ with the procedure outlined in section 2, based on a 15% loss-in-shielding criterion, it is difficult to see how the correct $\mathrm{d}H_{c1}/\mathrm{d}T$ could differ from the values of $\mathrm{d}H_{c1}^*/\mathrm{d}T$ in table 1 by more than a factor 2. For example, going over to a 3% loss-in-shielding criterion results in a $|\mathrm{d}H_{c1}^*/\mathrm{d}T|$ only about 30% smaller. One is therefore led to question the applicability of the standard one-κ GL description for this transition.

From a theoretical point of view, with the growing evidence in favour of a vector order parameter to describe phase A (high T, low H) of UPt_3, and the associated zeroes of the gap function which that implies, along with a possibly unconventional structure of the vortices [20], it appears not unlikely that the standard GL formulation would fail to account for the onset of that phase.

5. Conclusion

Our investigation of the low-field diamagnetic response in superconducting UPt_3 has revealed an increase in the slope of $H_{c1}(T)$ occurring at $T_0 = T_c^-$, i.e. precisely at the lower transition within the superconducting regime, giving support to the notion that this transition involves a new superconducting order parameter. An anomalously small Meissner effect was observed, corresponding to only 3% at most of the full flux expulsion, in a sample with long electronic mean free paths, and even though the vortices are otherwise known to move easily under the application of a Lorentz force. The initial slope of $H_{c1}(T)$ (near T_c^+) was found to be roughly isotropic, with a value rather

close to that of the thermodynamic critical field $H_c(T)$, in sharp contrast with the anisotropy and the much larger values of $-dH_{c2}/dT$. This unusual relation between the three critical fields, all determined experimentally, shows that the upper superconducting transition (from the normal state) cannot be described in the usual manner, with only one GL parameter κ, even near $T_c(H = 0)$. Finally, a comparison with the broken-symmetry model of Hess *et al* for the multicomponent phase diagram of UPt_3 reveals that the observed kink in $H_{c1}(T)$ at T_c^- is considerably less pronounced, and also less anisotropic than predicted, at least from the model in its simplest form.

References

[1] Taillefer L, Flouquet J and Lonzarich G G 1991 *Physica* B *Proc. LT 19 (Brighton, 1990)* vol III
[2] Hasselbach K, Taillefer L and Flouquet J 1989 *Phys. Rev. Lett.* **63** 93
[3] Hasselbach K, Lacerda A, de Visser A, Behnia K, Taillefer L and Flouquet J 1990 *Low Temp. Phys.* **81** 299
[4] Trappmann T, v Löhneysen H and Taillefer L 1991 *Phys. Rev.* B at press
[5] Taillefer L, Behnia K, Hasselbach K, Flouquet J, Hayden S M and Vettier C 1990 *J. Magn. Mater.* **90** & **91** 623
[6] Aeppli G, Bücher E, Broholm C, Kjems J K, Baumann J and Hufnagl J 1988 *Phys. Rev. Lett.* **60** 615
[7] Joynt R 1988 *Supercond. Sci. Technol.* **1** 210
[8] Hess D W, Tokuyasu T and Sauls J A 1989 *J. Phys.: Condens. Matter* **1** 8135
[9] Machida K, Ozaki M and Ohmi T 1989 *J. Phys. Soc. Jpn* **58** 4116
[10] Taillefer L and Lonzarich G G 1988 *Phys. Rev. Lett.* **60** 1570
[11] Keller N *MA thesis* CRTBT-CNRS, Grenoble, France
[12] Behnia K *PhD thesis* CRTBT-CNRS, Grenoble, France
[13] Adenwalla S, Lin S W, Zhao Z, Ran Q Z, Ketterson J B, Sauls J A, Taillefer L, Hinks D G, Levy M and Sarma B K 1990 *Phys. Rev. Lett.* **65** 2298
[14] Zhao Z, Behroozi F, Ketterson J B, Guan Y, Sarma B K and Hinks D G 1990 *Physica* B **165** & **166** 345
[15] Shivaram B S, Gannon J J Jr and Hinks D G 1989 *Phys. Rev. Lett.* **63** 1723
[16] Hess D W, Tokuyasu T A and Sauls J A 1990 *Physica* B **163** 720
[17] Taillefer L 1990 *Physica* B **163** 278
[18] Joynt R, Mineev V P, Volovik G E and Zhitomirsky M E 1990 *Phys. Rev.* B **42** 2014
[19] Tinkham M 1980 *Introduction to Superconductivity* (Malabar, FL: R E Krieger) p 156
Saint-James D and Sarma G 1969 *Type II Superconductivity* (Oxford: Pergamon Press) p 51
[20] Tokuyasu T A, Hess D W and Sauls J A 1990 *Phys. Rev.* B **41** 8891